

Pull-Off Behavior of Hand-Cast, Thermoformed, Milled, and 3D-Printed Splints

Verena Hickl, DS
Thomas Strasser, DDS
Alois Schmid, DDS
Martin Rosentritt, PhD

Department of Prosthetic Dentistry, UKR University Hospital Regensburg, Regensburg, Germany.

Purpose: To investigate the insertion/pull-out performance of splints produced by hand casting, thermoforming, milling, and 3D printing. **Materials and Methods:** A total of 120 identical mandibular splints ($n = 8$ specimens per group) were manufactured with hand casting, thermoforming, milling, and 3D printing. The splints were stored in water at 37°C for 10 days and then placed onto cobalt-chromium arches and fixed on one side. Forces were applied to the other side (centric, perpendicular 50 N, 1 Hz) at two different positions (teeth 46 and 44/45) to pull out, and the test was then reset. The number of pull-out cycles until failure was recorded. The fracture behavior of the splints was investigated and characterized as fracture in the loading position, fracture at the fixation, or combined fracture. Splints were pulled off until fracture as a control ($v = 1$ mm/minute). Finite element analysis was used to verify the results. Statistical analyses were conducted with one-way ANOVA, post hoc Bonferroni, Pearson correlation, and Kaplan-Meier log-rank tests ($\alpha = .05$). **Results:** The mean pull-off cycles varied from 7,839 (V-Print) to 1,600,000 (Optimill) at the tooth 46 position (FDI numbering system) and from 9,064 (Splint Comfort) to 797,750 (Optimill) at the 44/45 position. Log-rank test showed significantly ($P < .001$) different pull-out cycles between the systems (chi-square: 61,792 to 122,377). The thickness of the splints varied between 1.6 ± 0.2 mm (Splint Comfort) and 2.3 ± 0.1 mm (V-Print). Thickness and number of cycles were correlated (Pearson: 0.164; $P = .074$). The pull-off forces of the control varied significantly ($P \leq .040$), ranging from 13.0 N (Keysplint) to 82.2 N (Optimill) at the tooth 46 position and from 25.2 N (Keysplint) to 139.0 N (Optimill) at the 44/45 position. **Conclusions:** The milled and cast splints survived more pull-off cycles than the printed or thermoformed splints. The pull-out performance showed differences among the tested splint systems and indicated the influence of the material properties and processing. *Int J Prosthodont* 2024;37(suppl):s31–s40. doi: 10.11607/ijp.8068

In addition to physical, manual, and physiologic^{1,2} therapies, bite splints have been shown to be a noninvasive, reversible treatment option for temporomandibular disorders and craniomandibular disorders and for reducing tooth wear for patients with bruxism.^{3,4} An occlusal splint is used for the treatment of functional disorders and enables the testing of an occlusal or intermaxillary concept for definitive orthodontic, combined orthodontic-surgical, prosthetic, and/or restorative therapy. One goal is centric occlusion with neutral assignment of the anterior and posterior teeth, in accordance with the centric condylar position. An occlusal splint can be used for differential diagnostic clarification to protect the tooth structure from occlusal and incisal abrasion if the causal complaints are unclear.

Correspondence to:
Dr Martin Rosentritt,
martin.rosentritt@ukr.de

Submitted October 21, 2021;
accepted April 20, 2022.
©2024 by Quintessence
Publishing Co Inc.

Clinical failure of splints may result from discoloration, embrittlement/softening caused by water uptake, solubility, or fracture during handling or wear, all of which result in a loss of function.^{5–7} Brittle fractures, which frequently occur during splint insertion or removal, may cause oral injuries. Insertion and pull-off forces and lift-off height might be influenced by the design, fitting, and stability of the splint. Therefore, checking the fracture behavior of the splints during insertion and removal could be used to estimate the indication time.

Traditionally, adjusted splints⁵ are cast methacrylates or thermoformed thermoplastics on the basis of a laboratory-made gypsum model. A methacrylate splint, however, is limited in its clinical application due to its brittleness, polymerization shrinkage during manufacture, and residual monomers.^{8,9} Unlike methacrylate, thermoplastic foils (eg, polyethyleneterephthalate) provide easy fabrication and high flexibility but require occlusal material addition for therapeutic applications. CAD/CAM milling and 3D printing are alternative fabrication methods that allow easy and fast splint fabrication. They enable quick and inexpensive remanufacture in cases of fracture or need for adjustments to continue the clinical treatment (eg, bite adjustment).

Materials for CAD/CAM milling¹⁰ are produced under controlled industrial conditions with heat and pressure. Therefore, they have improved mechanical properties and reduced residual monomer content but also show brittleness. When milling, the size of the drill affects the fit and roughness of the inner sides of the splint.¹¹ Milled splints showed good performance in pull-off tests.¹²

Digital light processing vat 3D-printing technologies^{10,13–15} use liquid photopolymer resins that are cured by a light projector during splint construction. A proper alignment of the material and processes^{16,17} is crucial for optimizing the printing processes, requiring an appropriate viscosity for the resin, for example.⁶ 3D-printed splints show acceptable accuracy^{18,19} but often limited conversion.²⁰ Therefore, after printing and subsequent cleaning, the splints are finalized in a postpolymerization process using external light curing devices, sometimes combined with heat and vacuum treatment.^{12,17} In comparison with milled or hand-cast systems, 3D-printed splints may have lower mechanical properties, combined with worse results in application-related pull-off tests.¹² However, the targeted use of greater splint flexibility can, for example, contribute to improved wearing comfort and better friction.

Even though splints are widely used, research on the performance of conventional or particularly new systems is very limited. Before introducing new materials, their mechanical stability^{10,21,22} should be checked, but the influences of aging or clinical interactions should also be tested.¹² In contrast to tests on simple test specimen geometries, component testing on splints might help

verify the clinical failures,²³ taking into account the respective types of production and design. In vitro testing and finite element analysis can be used to understand how splints can fail during insertion/pull-off.^{24–26} However, in vitro tests on standardized specimens can only provide a clinical assessment and cannot replace clinical studies, as individual patient-specific parameters, such as masticatory force or jaw movement, cannot be taken into account.

It can be assumed that different materials and manufacturing processes should influence the in vitro performance and pull-off force of splints. In addition, the clinical application (ie, how often and how the splint is inserted or removed) certainly plays a decisive role in its service life.

The first hypothesis of this in vitro study was that hand-cast, thermoformed, milled, and 3D-printed splints would show identical in-vitro pull-off performance and force. The second hypothesis was that the position of the force application would have no effect on the in vitro pull-off performance and force.

MATERIALS AND METHODS

A total of 120 (8 × 15) identical mandible splints (second molar to second molar; teeth 37 to 47 [FDI numbering system]), which were based on an STL (standard tessellation language) file, were manufactured from various materials and material combinations (n = 8 per testing group), representing actual splint fabrication procedures: hand-casting (reference), thermoforming, CAD/CAM milling, and 3D printing.

Table 1 lists all of the materials, manufacturers, and methods for creating the splints used in the present study. Printed splints were created from splint materials LuxaPrint Ortho Plus (printed via Cares P30+), KeySplint Soft (printed via Cares P30), and V-Print Splint and Splint Comfort (both printed via SolFlex 650). Printing was performed at a 90-degree angle to the building platform in 50- μ m layers with supporting structures. Specimens were either automatically cleaned (P Wash, Straumann) or manually washed (2-minute isopropanol bath and ultrasonic cleanser). Postpolymerization was performed with LED (light-emitting diode) or xenon light (Otoflash G171). Milled splints (Optimill Crystal Clear) were processed via Zenotec Select Ion, and thermoformed splints (Erkodur) were processed via Erkoform 3D Motion. The hand-cast system (Palapress Varop transparent) was manufactured in a pressure pot (55°C, 2 bar, 15 minutes). The surface of the splints was finished (pumice powder with a goat hair brush, polymer polish with a cotton brush) before testing. The inner sides were left as manufactured to guarantee the required friction.

The splints are usually removed and reinserted several times a day for cleaning or eating. As a result, they are subjected to repeated loads (eg, bending) and are prone

Table 1 Materials and Fabrication

System	Material (manufacturer)	Lot no.	Processing	Composition, properties
Thermoforming	Erkodur, 2.00 mm, 120 mm (Erkodent)	111888/11307	Erkoform 3D Motion (Erkodent)	Polyethyleneterephthalate PET-G Flexural strength: 69 MPa Water uptake: 1.27 g/cm ³ Flexural modulus: 2.2 GPa
Hand-cast system MA	Palapress Vario transparent (Kulzer)	K010201/K010089	Pressure pot (55°C, 2 bar, 15 min)	Powder: Methacrylate copolymer Liquid: methacrylate, Di-methacrylate Flexural strength: 82.9 MPa Flexural modulus: 2.5 GPa Water uptake: 21.6 µg/mm ³ Solubility: 0.4 µg/mm ³
Milling	Optimill Crystal Clear (Dentona)	20040	Zenotec Select Ion (Wieland Dental Systems); Spacer: 30 µm Undercut: 0.1 mm Correction radius: 1.1 mm	Polymethylmethacrylate, Methylmethacrylate, Dibenzoylperoxide, Methyl 2-methylprop-2-enoate Flexural strength: 95 MPa Flexural modulus: 2.39 GPa Water uptake: < 30 µg/mm ³ No solubility in water
Print	LuxaPrint-Ortho Plus (DMG America)	170211	Cares P30+ (Straumann) <i>Printing:</i> direction: 90 degrees to building platform; layer: 50 µm <i>Cleaning:</i> P wash (Straumann), isopropanol <i>Polymerization:</i> P Cure (Straumann) LED	Dimethacrylate, EBPADMA, Diphenyl(2,4,6-trimethylbenzoyl) phosphine oxide (> 90% bisphenol A dimethacrylate, 385/405 nm Flexural strength: ≥ 70 MPa Flexural modulus ≥ 1 GPa Shore D: ≥ 60
Print	KeySplint Soft (Keystone Industries)	K84189		Methacrylate Flexural strength: 48 MPa Flexural modulus: ~0.75 GPa
Print	V-Print Splint (VOCO)	2006565	SolFlex 650 (VOCO) <i>Printing:</i> direction: 90 degrees to building platform; layer: 50 µm <i>Cleaning:</i> ultrasonic (2 min), isopropanol <i>Polymerization:</i> xenon light (OtoFlash G171) at 2*2,000 flashes	Acrylate, Bis-EMA, TEGDMA, hydroxypropyl methacrylate Flexural strength: 75 MPa Flexural modulus: ≥ 2.1 GPa Water uptake: 27.7 µg/mm ³ Solubility: < 0.1 µg/mm ³ butylated hydroxytoluene BHT, diphenyl(2,4,6-trimethylbenzoyl) phosphine oxide TPO, 385 nm)
Print	Splint Comfort (VOCO)	V87146		Flexural strength: 55 MPa Flexural modulus: ~0.8 GPa

to fracture. The tests were designed to simulate splint insertion/removal at two different splint positions. Metal-based (cobalt-chromium [CoCr]) standardized mandibles were produced via selective laser melting for the insertion/pull-off tests. The splints were fabricated with an undercut and fixed onto the metal mandible, simulating the clinical situation. Each test splint was identical to the master splint and was individually controlled on the master model to ensure identical undercuts. Each undercut was evaluated by the same person (V.H.) to standardize this assessment and show comparable results. A metal plate was screwed onto the splint, fixing the complete side of the splint firmly onto the metal mandible from tooth positions 31 to 37 (FDI numbering system).

To investigate two different pull-off situations, a screw was polymerized onto the mandible for fixation of the pull-off mechanism at tooth position 44/45 or 46 (Fig 1). Cyclic pull-off and insertion forces (EGO chewing

simulator, Regensburg; centric, perpendicular 50 N, 1 Hz, pneumatic) were applied to pull off the splint on one side by 3 mm. Forces were applied via a flexible rubber trigger mechanism to avoid shear and bending forces on the splint. Before testing, all specimens were stored in distilled water for 10 days at 37°C, allowing for aging and water absorption.¹⁰ During the insertion/pull-off tests, simultaneous thermal cycling (TC) between 5°C and 55°C (2 minutes each temperature) was performed for additional aging and to avoid dry-out of the splints. To investigate the principal effect of TC, one material (Luxa Print OrthoPlus) was investigated without TC.

During the tests, samples were checked for failures three times a day, and damaged specimens were excluded from further simulation. Cycles until fracture (number of insertion/pull-off cycles) were recorded. Failures were characterized according to the tooth location, and the failure mode was documented (evaluated via digital



Fig 1 Experimental setup. (a) Cyclic pull-off testing chamber with splint, occlusal fixation, and vertical pull-off fixation. (b) Fracture test.

microscope [VHX, Keyence] at $\times 50$ magnification). Failure patterns were categorized as a fracture in the position of loading (tooth 46 or 44/45), fracture at the fixation (tooth 31), or a combined fracture (multiple). The splint thickness was measured in the area of the fracture and at the back end of the splint (control). Finite element analysis (Fusion 360, Autodesk) was performed based on the STL file of the splint to verify the failure performance during testing. Before conducting the repeated testing, pull-off tests perpendicular to the occlusal surface of the splints were performed in a universal testing machine ($v = 1$ mm/minute; Z010, ZwickRoell) on two splints from each group to determine maximum pull-off forces (see Fig 1).

Means and standard deviations were calculated. Differences between mean values were analyzed using uni-/bivariate analysis of variance and ANOVA. Correlations between the individual groups were investigated (Pearson). Levene's test was performed to check for the error variance of the dependent variable across groups. Cumulative survival was calculated using Kaplan-Meier log rank (Mantel-Cox) test (SPSS version 25.0, IBM). The level of significance was set to $\alpha = .05$.

RESULTS

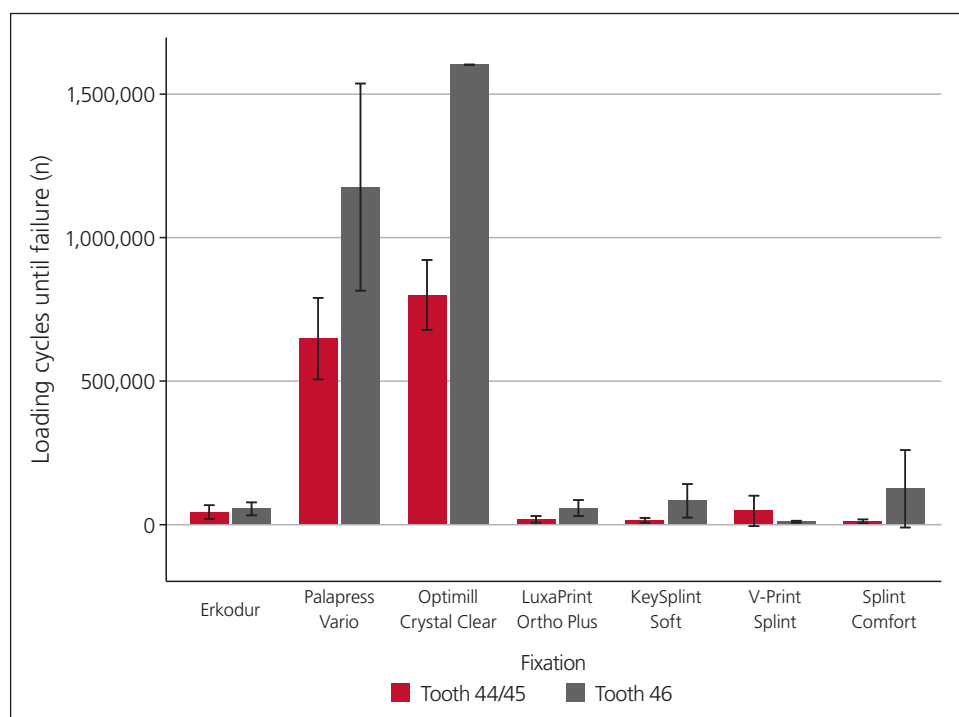
Table 2 lists the number of loading cycles until fracture and the results of pull-off test load to fracture for all materials used. Fractures occurred at mean pull-off forces between 13.0 N (KeySplint) and 82.2 N (Optimill) at the loading position of tooth 46, and between 25.2 N (Splint Comfort) and 139.0 N (Optimill) at the loading position of tooth 44/45. Splints that were loaded in position 46 showed comparable or lower fracture values. Differences

between the individual failure forces were significant ($P \leq .040$). Optimill specimens in loading in position tooth 46 survived the pull-off/insertion tests. The fracture force of these specimens was 49.0 ± 19.9 N.

The mean pull-off cycles to failure varied between 7,839 cycles (V-Print) and 1,600,000 cycles (Optimill) for fixation in tooth position 46, and between 9,064 cycles (Splint Comfort) and 797,750 cycles (Optimill) for fixation in tooth position 44/45 (Figs 2 and 3; see also Table 2). Only Optimill splints in tooth position 46 survived the cycling tests and were loaded to failure in the pull-off test. Splint fracture during the insertion/pull-off test was characterized by brittle fracture between the loading position (38 times at tooth position 44/45, 44 times at tooth position 46), at the fixation point (8 times for position 44/45, 7 times for position 46), or multiple fracture (10 times for position 44/45, 5 times for position 46) (Fig 4). Finite element method (FEM) analysis showed that the fracture was triggered at the bottom side of the splint in the loading position or the fixation point (Fig 5). Log-rank test showed significantly ($P = .000$) different insertion/pull-off cycles between the systems (chi-square = 61,792 to 122,377; degree of freedom: 6) for both loading positions (see Fig 1). For the TC control (Luxa Print), the influence of TC on the number of cycles was found to be insignificant (chi-square = 0.395; $P = .530$). Splint thickness varied between 1.6 ± 0.2 mm (Splint Comfort) and 2.3 ± 0.1 mm (V-Print Splint) (Fig 6). Pearson's chi-square test showed a correlation between the number of cycles and the thickness (0.164; $P = .074$). A significant correlation was found between the number of cycles and the pull-off force (0.623; $P = .170$) in loading position 46, but no correlation (0.713; $P = .040$) was noted for loading position 44/45. See Fig 3

Table 2 Number of Loading Cycles Until Failure in the Pull-Off Test Load to Fracture

Material	Fixation tooth 46						Fixation tooth 44/45					
	Loading cycles until failure, n				Fracture force, N		Loading cycles until failure, n				Fracture force, N	
	Mean	SD	Min	Max	Mean	SD	Mean	SD	Min	Max	Mean	SD
Erkodur	41,315	23,733	655	67,180	62.5	29.1	52,328	22,574	18,562	76,025	95.4	3.3
Palapress Vario	645,516	142,026	346,125	839,000	62.3	29.6	1,173,542	360,768	748,185	1,502,150	81.8	22.1
Optimill Crystal Clear	797,750	121,897	643,500	1,019,000	82.2	18.2	1,600,000	0	1,600,000	16,00,000	139.0	18.4
LuxaPrint Ortho Plus	15,967	11,438	5,046	31,135	50.3	6.7	63,976	17,638	42,698	7,7982	50.1	1.6
KeySplint Soft	12,719	8,353	163	24,761	13.0	2.1	80,421	58,374	9,824	160,513	35.4	26.0
V-Print Splint	45,447	53,101	38	128,823	34.0	0.0	7,839	3,453	26	9,891	32.5	5.0
Splint Comfort	9,064	6,675	1,212	18,367	18.2	3.8	122,370	134,839	19,267	329,623	25.2	6.2

Fig 2 Loading until failure values (means \pm SDs) for each material tested.

and Table 2 for the cumulative survival times and failure patterns.

DISCUSSION

The first hypothesis of this in vitro study, which stated that hand-cast, thermoformed, milled, and 3D-printed splints would show different in-vitro pull-off performance, could not be confirmed. Milled and hand-cast

splints showed higher mean survival rates and higher pull-off forces than printed or thermoformed systems.

The second hypothesis, which stated that the position of the force application would not affect the in vitro pull-off performance, must be rejected. In general, the splints lasted longer when the loading was applied at position tooth 46. Printed and thermoformed splints showed different rankings in different loading positions.

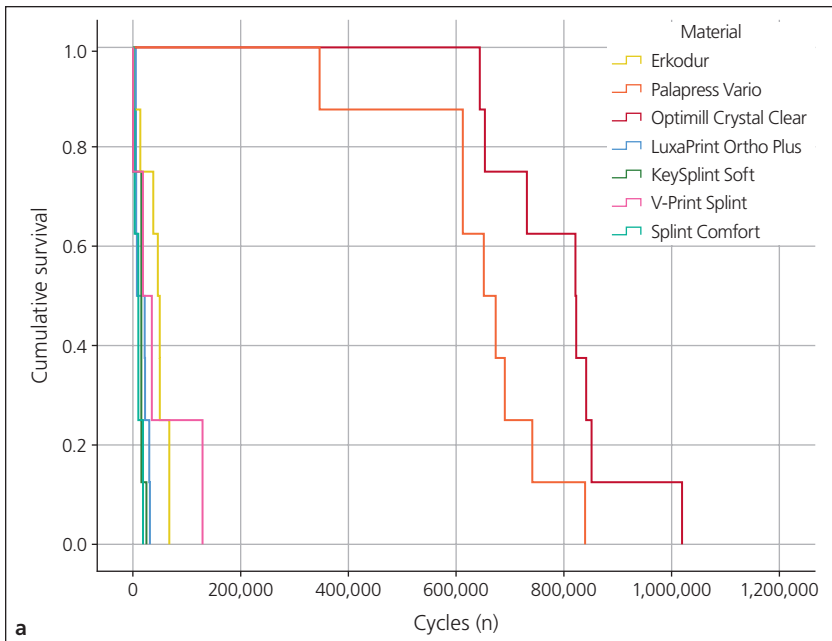
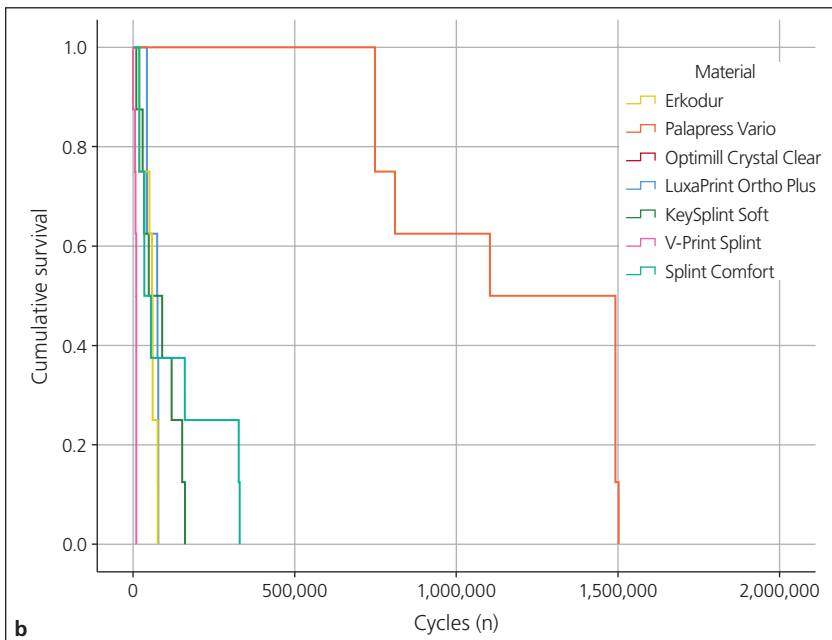


Fig 3 Kaplan-Meier cumulated survival of the individual splint materials at (a) position 44/45 and (b) position 46.



The different in vitro behavior of the investigated splint materials can be partly explained by the individual material properties. The longest survival in both loading situations was found with highest the modulus of elasticity (~2.4 GPa) and flexural strength (~82 MPa). Milled materials showed comparable or even improved properties in comparison to standard methacrylate,¹⁰ confirming their comparable or better performance. 3D-printed materials generally provide lower flexural strength and modulus of elasticity. Particularly flexible and soft materials naturally and intentionally have even lower values (see manufacturer information in Table 1).

The low mean survival rates of the printed splints can be attributed to the composition of the resin systems and the resulting lower flexural strength and modulus of elasticity. For 3D printing, a low-viscosity formulation is needed, which guarantees workability in the printer. Fillers that could improve the strength and E-modulus²⁷ can be added only in small amounts because they would limit the printability of the materials too much. In addition, an absence of chemical curing ingredients, which would improve the conversion rate and thus also the strength,^{20,28–30} may be a reason for lower survival rates. By optimizing the positioning and

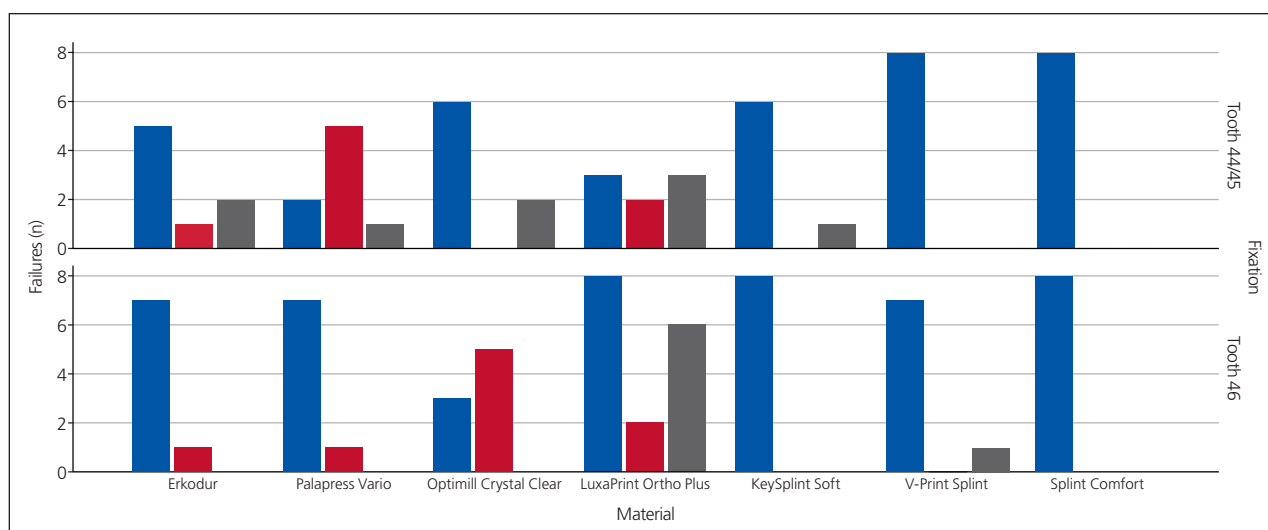
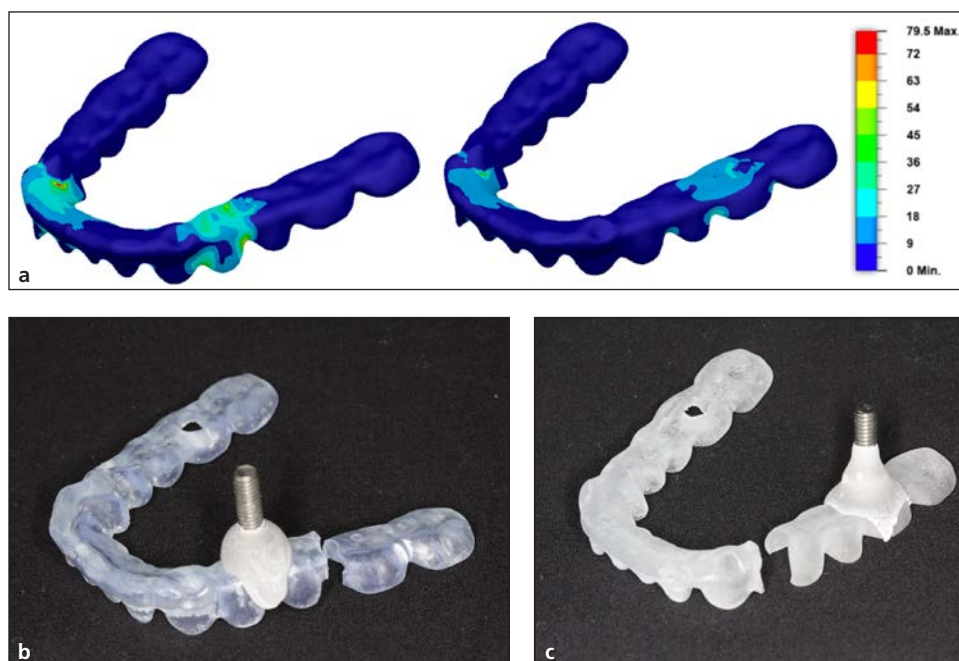


Fig 4 Failure pattern of the splints after pull-off testing. *Optimill is the exception, as tooth 46 was evaluated after static testing. Bar color indicates failure pattern: blue = loading; red = fixation; gray = multiple.

Fig 5 (a) FEM analysis at loading position tooth 44/45 (left) and position 46 (right), showing locations with highest von Mises stress (MPa) in the loading position or the anterior fixation. (b and c) Splints with the loading positions at site 44/45 and site 46, respectively, used for evaluation.



alignment of the splint,^{17,31} the survival time might be improved.^{16,32}

The high standard deviations seen in the present results may be a result of variations in the material quality or the influence of the fabrication.^{32,33} Individual failures, especially of the printed materials occurring during a very early stage of the test, might be explained by superficial defects or roughness effects due to printing and may underline the necessity of cleaning, postpolymerization, and polishing.^{12,34} This assumption might be confirmed by the fact that considerably longer survival rates were

found for other specimens from the same groups. In a similar study,¹² significantly lower survival cycles could be determined in a comparable loading situation (tooth 46, 12-mm pull-off height).¹² Contrary to the current study, thermoformed and hand-cast systems showed longer survival times than printed or milled splints.¹² This is probably attributed to the significantly higher pull-off height (12 mm) in the previous study compared to the 3-mm pull-off height applied in the present study and shows how the results are affected by the test design.

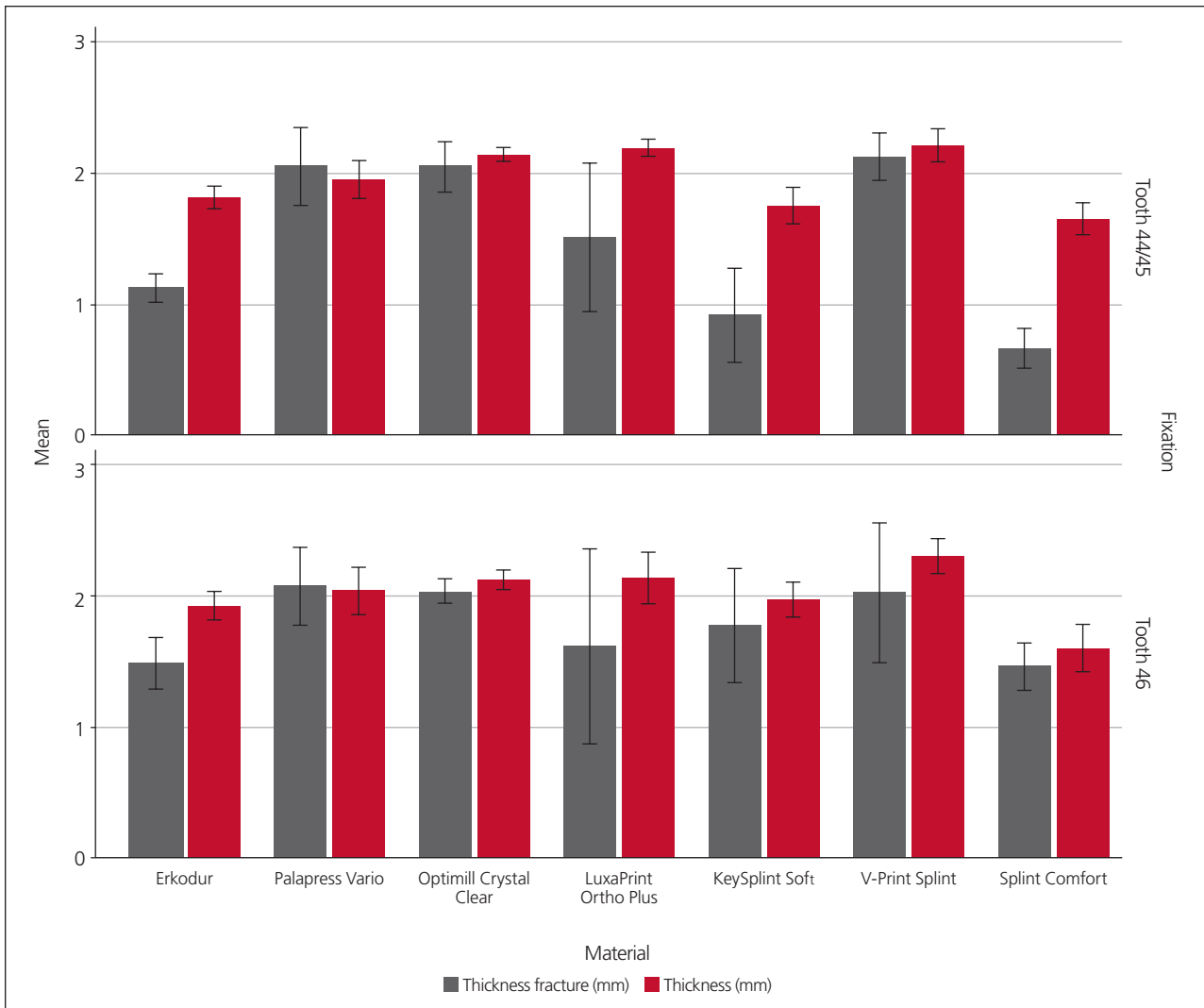


Fig 6 Splint thickness in the area of fracture and at the back end. Values are presented in millimeters as mean \pm SD.

Although based on one identical model, the thickness at the back end of the splints varied noticeably, between 1.6 and 2.3 mm. Despite being based on identical data, three of the four printed splints and the thermoformed system were significantly thinner than the milled or hand-cast splints, which indicates the influence of the printing process or the postfabrication procedure. It is also conceivable that material was removed during the cleaning process. Deviations can certainly appear due to the different production processes and corresponding tolerances, as reported previously.¹² Different thicknesses at the fracture area might be attributed to thinning and aging effects (fracture of the polymeric chains) at the loading point. A correlation between the number of cycles and the splint thickness could be proven in the present study. The present results suggest that adapted thickness, as well as adapted postprocessing, can extend the lifespan of splints.

Assuming a mean of three insertions and removals per day, 1,095 pull-off cycles are required to simulate 1 year of oral service. It is expected that these splints will be usable for at least a few years. However, the minimum load cycles with values between 16 and 655 cycles to failure indicate that individual splints could fail much earlier. Nevertheless, due to the estimated occlusal wear of resin-based splint materials,^{5-7,35} such a long application time is not anticipated.

The materials showed different pull-off forces, with the lowest values found for the soft or flexible printing materials, followed by the standard printing materials, then thermoformed or hand-cast systems. The highest values were found for the milled splints. Compared to the hand-cast systems, the milled system had an enhanced performance expressed by a longer application time and a smaller distribution of defect sites. One explanation could be the influence of the industrial processing of



the material,^{19,36} resulting in improved conversion and mechanical stability. For example, the E-modulus is significantly affected by thermoforming.³⁷ For five out of seven investigated materials, differences in the fracture force could be found depending on the loading situation. At position 44/45, the forces were significantly higher. This may be explained by the lower deflection/shorter lifting arm at position 46 compared to position 44/45. For the acrylate-based systems, there appears to be a relationship between the pull-off force and the flexural strength, but not with the modulus of elasticity. The pull-off test leads to an effective aging of the splints, which results in a significant reduction of the pull-off force (as seen for Optimill). A correlation between the number of cycles and the fracture load was confirmed. Due to the small number of cases, the forces must be evaluated with caution.

By analyzing the failure pattern and performing a finite element analysis, it was determined that a fracture is caused by the high deflection and repeated bending at the lower side of the splint. A fracture may be more likely to occur in these areas if there are sharp edges or initial damage.¹² According to the modulus of the material, the fracture pattern might be brittle or flexible. The fracture toughness of the material and the intaglio surface¹¹ influenced by the milling process must be considered. The fracture behavior was characterized in most cases by a fracture in the area of the loading site, followed by fractures in the area of the anterior fixation. These results confirmed earlier data and followed the expectations presented in the FEM. For the printed splints, the distribution of fracture patterns may indicate fabrication defects or insufficiently connected print layers.^{16,32} The evaluation of Optimill at tooth 46 is only possible to a limited extent, as all specimens survived the pull-off test and were then manually loaded to fracture. In addition to typical signs of aging, an influence and weakening of the splint caused by the manual fixation of the mount with methacrylate could not be excluded. An alternative cause of damage in region 35 might be too strong of a splint retention on the metal model. All systems showed brittle fractures during pull-off, which poses a clinical risk for injury. Patients should be careful when repeatedly removing their splints to prevent fractures. The FEM and the assessment of the fracture patterns suggest that the bottom side of all splints should also be inspected for defects before use. To improve their clinical performance, polishing (paying attention to the walls) and cleaning might be of particular importance to avoid undesirable splint fracture.

CONCLUSIONS

The pull-off performance of the splints is highly influenced by the type of material and the manufacturing


process. Loading at tooth position 46 results in longer loading cycles for almost all materials. Pull-off tests showed that milled and hand-cast splints provided the longest survival. If a very long duration of use is needed, these materials are to be preferred. Printed and thermoformed splints showed comparable but 10-fold lower survival times than milled and hand-cast splints.

ACKNOWLEDGMENTS

The authors would like to thank individual manufacturers for providing materials. This research did not receive any specific grant from funding agencies in the public, commercial, or not-for-profit sectors. The authors report no conflicts of interest.

REFERENCES

1. Akbulut N, Altan A, Akbulut S, Atakan C. Evaluation of the 3 mm thickness splint therapy on temporomandibular joint disorders (TMDs). *Pain Res Manag* 2018;2018:3756587.
2. Behr M, Stebner K, Kolbeck C, Faltermeier A, Driemel O, Handel G. Outcomes of temporomandibular joint disorder therapy: Observations over 13 years. *Acta Odontol Scand* 2007;65:249–253.
3. Riley P, Glenny AM, Worthington HV, et al. Oral splints for patients with temporomandibular disorders or bruxism: A systematic review and economic evaluation. *Health Technol Assess* 2020;24:1–224.
4. Crout DK. Anatomy of an occlusal splint. *Gen Dent* 2017;65:52–59.
5. Lutz AM, Hampe R, Roos M, Lümekemann N, Eichberger M, Stawarczyk B. Fracture resistance and 2-body wear of 3-dimensional-printed occlusal devices. *J Prosthet Dent* 2019;121:166–172.
6. Kessler A, Reymus M, Hickel R, Kunzelmann KH. Three-body wear of 3D printed temporary materials. *Dent Mater* 2019;35:1805–1812.
7. Reyes-Sevilla M, Kuijs RH, Werner A, Kleverlaan CJ, Lobbezoo F. Comparison of wear between occlusal splint materials and resin composite materials. *J Oral Rehabil* 2018;45:539–544.
8. Ben Hassan MW, Andersson L, Lucas PW. Stiffness characteristics of splints for fixation of traumatized teeth. *Dent Traumatol* 2016;32:140–145.
9. Berthold C, Auer FJ, Potapov S, Petschelt A. In vitro splint rigidity evaluation—Comparison of a dynamic and a static measuring method. *Dent Traumatol* 2011;27:414–421.
10. Berli C, Thieringer FM, Sharma N, et al. Comparing the mechanical properties of pressed, milled, and 3D-printed resins for occlusal devices. *J Prosthet Dent* 2020;124:780–786.
11. Lebon N, Tapie L, Vennat E, Mawussi B. Influence of CAD/CAM tool and material on tool wear and roughness of dental prostheses after milling. *J Prosthet Dent* 2015;114:236–247.
12. Rosentritt M, Behr M, Strasser T, Schmid A. Pilot in-vitro study on insertion/removal performance of hand-cast, milled and 3D printed splints. *J Mech Behav Biomed Mater* 2021;121:104612.
13. Dedem P, Türp JC. Digital Michigan splint—From intraoral scanning to plasterless manufacturing. *Int J Comput Dent* 2016;19:63–76.
14. Pagac M, Hajnys J, Ma QP, et al. A review of vat photopolymerization technology: Materials, applications, challenges, and future trends of 3D printing. *Polymers (Basel)* 2021;13:598.
15. Wedekind L, Güth JF, Schweiger J, et al. Elution behavior of a 3D-printed, milled and conventional resin-based occlusal splint material. *Dent Mater* 2021;37:701–710.
16. Alharbi N, Osman R, Wismeijer D. Effects of build direction on the mechanical properties of 3D-printed complete coverage interim dental restorations. *J Prosthet Dent* 2016;115:760–767.
17. Rosentritt M, Huber C, Strasser T, Schmid A. Investigating the mechanical and optical properties of novel urethandimethacrylate (UDMA) and urethanmethacrylate (UMA) based rapid prototyping materials. *Dent Mater* 2021;37:1584–1591.

- 
18. Nestler N, Wesemann C, Spies BC, Beuer F, Bumann A. Dimensional accuracy of extrusion- and photopolymerization-based 3D printers: In vitro study comparing printed casts. *J Prosthet Dent* 2021;125:103–110.
 19. Reymus M, Fabritius R, Keßler A, Hickel R, Edelhoff D, Stawarczyk B. Fracture load of 3D-printed fixed dental prostheses compared with milled and conventionally fabricated ones: The impact of resin material, build direction, post-curing, and artificial aging—An in vitro study. *Clin Oral Investig* 2020;24:701–710.
 20. Alifui-Segbaya F, Bowman J, White AR, George R, Fidan I. Characterization of the double bond conversion of acrylic resins for 3D printing of dental prostheses. *Compend Contin Educ Dent* 2019;40:e7–e11.
 21. Perea-Lowery L, Gibreel M, Vallittu PK, Lassila L. Evaluation of the mechanical properties and degree of conversion of 3D printed splint material. *J Mech Behav Biomed Mater* 2021;115:104254.
 22. Grymak A, Aarts JM, Ma S, Waddell JN, Choi JJE. Comparison of hardness and polishability of various occlusal splint materials. *J Mech Behav Biomed Mater* 2021;115:104270.
 23. Rosentritt M, Behr M, van der Zel JM, Feilzer AJ. Approach for valuating the influence of laboratory simulation. *Dent Mater* 2009;25:348–352.
 24. Tahayeri A, Morgan M, Fugolin AP, et al. 3D printed versus conventionally cured provisional crown and bridge dental materials. *Dent Mater* 2018;34:192–200.
 25. Zimmermann M, Ender A, Egli G, Özcan M, Mehl A. Fracture load of CAD/CAM-fabricated and 3D-printed composite crowns as a function of material thickness. *Clin Oral Investig* 2019;23:2777–2784.
 26. Lee WS, Lee DH, Lee KB. Evaluation of internal fit of interim crown fabricated with CAD/CAM milling and 3D printing system. *J Adv Prosthodont* 2017;9:265–270.
 27. Koenig A, Schmidtke J, Schmohl L, et al. Characterisation of the filler fraction in CAD/CAM resin-based composites. *Materials (Basel)* 2021;14:1986.
 28. Arslan M, Murat S, Alp G, Zaimoglu A. Evaluation of flexural strength and surface properties of prepolymerized CAD/CAM PMMA-based polymers used for digital 3D complete dentures. *Int J Comput Dent* 2018;21:31–40.
 29. Kowalska A, Sokolowski J, Bociong K. The photoinitiators used in resin based dental composite—A review and future perspectives. *Polymers (Basel)* 2021;13:470.
 30. Navaruckiene A, Bridziuviene D, Raudoniene V, Rainosalo E, Ostrauskaite J. Influence of vanillin acrylate-based resin composition on resin photocuring kinetics and antimicrobial properties of the resulting polymers. *Materials (Basel)* 2021;14:653.
 31. Nold J, Wesemann C, Rieg L, et al. Does printing orientation matter? In-vitro fracture strength of temporary fixed dental prostheses after a 1-year simulation in the artificial mouth. *Materials (Basel)* 2021;14:259.
 32. Väyrynen VOE, Tanner J, Vallittu PK. The anisotropy of the flexural properties of an occlusal device material processed by stereolithography. *J Prosthet Dent* 2016;116:811–817.
 33. Gibreel M, Perea-Lowery L, Vallittu PK, Lassila L. Characterization of occlusal splint materials: CAD-CAM versus conventional resins. *J Mech Behav Biomed Mater* 2021;124:104813.
 34. Reymus M, Stawarczyk B. In vitro study on the influence of postpolymerization and aging on the Martens parameters of 3D-printed occlusal devices. *J Prosthet Dent* 2021;125:817–823.
 35. Grymak A, Aarts JM, Ma S, Waddell JN, Choi JJE. Wear behavior of occlusal splint materials manufactured by various methods: A systematic review. *J Prosthodont* 2022;31:472–487.
 36. Reymus M, Stawarczyk B. Influence of different postpolymerization strategies and artificial aging on hardness of 3D-printed resin materials: An in vitro study. *Int J Prosthodont* 2020;33:634–640.
 37. Golkhani B, Weber A, Keilig L, Reimann S, Bourauel C. Variation of the modulus of elasticity of aligner foil sheet materials due to thermoforming. *J Orofac Orthop* 2022;83:233–243.